



Published in final edited form as:

Top Stroke Rehabil. 2009 ; 16(4): 270–281. doi:10.1310/tsr1604-270.

Changes in Resting State Effective Connectivity in the Motor Network Following Rehabilitation of Upper Extremity Poststroke Paresis

G. Andrew James, PhD,

Research Associate and Faculty of the Wallace H. Coulter Department of Biomedical Engineering at Emory University and the Georgia Institute of Technology, Atlanta, Georgia

Zhong-Lin Lu, PhD,

William M. Keck Chair in Cognitive Neuroscience, Professor of Psychology & Biomedical Engineering, University of Southern California, Los Angeles, California

John W. VanMeter, PhD,

Associate Professor of Neurology, Georgetown University, Washington, DC

K. Sathian, MD, PhD,

Professor of Neurology, Psychology and Rehabilitation Medicine, Emory University, and Medical Director, Atlanta Veterans Affairs Medical Center, Atlanta, Georgia

Xiaoping P. Hu, PhD, and

Professor of the Wallace H. Coulter Department of Biomedical Engineering at Emory University and the Georgia Institute of Technology, and Director of the Biomedical Imaging Technology Center at Atlanta, Georgia

Andrew J. Butler, PT, PhD, FAHA

Associate Professor of Rehabilitation Medicine, Emory University, and Research Scientist, Atlanta Veterans Affairs Medical Center, Atlanta, Georgia

Abstract

Background—A promising paradigm in human neuroimaging is the study of slow (<0.1 Hz) spontaneous fluctuations in the hemodynamic response measured by functional magnetic resonance imaging (fMRI). Spontaneous activity (i.e., resting state) refers to activity that cannot be attributed to specific inputs or outputs, that is, activity intrinsically generated by the brain.

Method—This article presents pilot data examining neural connectivity in patients with poststroke hemiparesis before and after 3 weeks of upper extremity rehabilitation in the Accelerated Skill Acquisition Program (ASAP). Resting-state fMRI data acquired pre and post therapy were analyzed using an exploratory adaptation of structural equation modeling (SEM) to evaluate therapy-related changes in motor network effective connectivity.

Results—Each ASAP patient showed behavioral improvement. ASAP patients also showed increased influence of the affected hemisphere premotor cortex (*a*-PM) upon the unaffected hemisphere premotor cortex (*u*-PM) following therapy. The influence of *a*-PM on affected hemisphere primary motor cortex (*a*-M1) also increased with therapy for 3 of 5 patients, including those with greatest behavioral improvement.

Conclusions—Our findings suggest that network analyses of resting-state fMRI constitute promising tools for functional characterization of functional brain disorders, for intergroup comparisons, and potentially for assessing effective connectivity within single subjects; all of which have important implications for stroke rehabilitation.

Keywords

effective connectivity; fMRI; hemiparesis; motor cortex; physical therapy; resting state; structural equation modeling

According to the American Heart Association and the Centers for Disease Control and Prevention, stroke continues to be the third leading cause of death and is the leading cause of severe, long-term disability in the United States.¹ Every year, approximately 700,000 people suffer a stroke. Many of these survivors will have compromised ability to use their hemiparetic upper extremity in activities of daily life.

An understanding of the complex neural interactions underlying motor function may improve treatment efficacy. Toward this aim, neuroimaging has greatly enhanced our understanding of the motor system. Early positron emission tomography (PET) studies in humans have implicated (to varying extents) the sensorimotor cortex, premotor cortex, supplementary motor area, superior parietal cortex, striatum, and cerebellum in motor execution, planning, and learning.²⁻⁵ Over the past decade, functional magnetic resonance imaging (fMRI) has improved upon this corpus of knowledge with finer anatomic and temporal resolution. For example, fMRI has localized the region responsible for motor output of the hand to a distinct anatomic landmark along the precentral gyrus now known as the hand knob.⁶

Connectivity Analyses

Early neuroimaging analyses emphasized the magnitude or reliability of neural activation during a task. Height statistics (such as *t* tests) comparing activation magnitudes across conditions are important for determining what brain regions are activated during a task. Unfortunately, these statistics neglect the rich temporal information offered by fMRI. Using just these comparisons, it is difficult to determine if two neural regions are acting in concert as part of a single network or independently as components of two concurrent yet separate networks. An excellent example of this ambiguity lies in early motor learning neuroimaging research, where the contribution of various neural regions to motor execution, planning, and learning was difficult to tease apart using height statistics alone.²⁻⁵

Connectivity analyses offer additional information for resolving this quandary. While height statistics can determine what regions are involved in a task, connectivity analyses can determine how these regions interact. Functional connectivity can be inferred from the temporal correlation between activity in various brain regions. If the timecourses for regions A and B are consistently correlated during a task, then A and B are presumed to be components of the same network. Region C may also be activated during the task but is presumed to be part of a different network if not correlated with A or B. For example, Toni et al⁷ used functional timecourses of motor regions during a motor learning paradigm to determine what regions were involved in different stages of learning. Their graphical depictions of left dorsolateral prefrontal cortex, anterior cingulate, and left premotor cortex timecourses show strong correlation (particularly when contrasted to other regions, such as supplementary motor area); furthermore, these activity timecourses are greatest during motor learning and return to baseline for overlearned sequences. Thus, we infer that these regions are constituents of a network specialized for motor skill acquisition.

Several methods exist for applying connectivity analyses. The simplest is seed analysis, where one region's timecourse is used as a regressor against which all other regions' timecourses are correlated. Seed analyses produce statistical parametric maps indicating how strongly each region is correlated with the seed region. Seed analyses have been used widely in the functional connectivity literature, for example, to dissociate activity of Broca's and Wernicke's areas during overt speech, silent speech, and tongue movement.⁸ Seed analyses are by nature univariate; each analysis uses just one seed as a regressor. Multivariate connectivity analyses offer even richer interpretations, since these methods can incorporate two or more independent variables simultaneously. The subset of multivariate methods most commonly encountered in connectivity analyses includes component analyses, which seek to reduce the neural regions into networks that explain large percentages of the regions' temporal variability. These methods include principal component analysis,^{9,10} partial least squares,¹¹ and independent component analysis.^{12,13}

The techniques described thus far characterize *functional connectivity*, the correlated activity among brain regions. A growing emphasis has been placed upon *effective connectivity*, the influences neural regions have upon each other. While functional connectivity assesses the strength of correlation between brain regions, effective connectivity determines the directionality of these influences. Structural equation modeling (SEM) is the method most frequently used to model effective connectivity. SEM infers plausible directional connections among variables based upon their observed covariance. Early work demonstrated modulation of acoustic pathways in rats during habituation,¹⁴ modulation of V5's influence on posterior parietal cortex by prefrontal cortex during attention,¹⁵ and increasing influence of posterior parietal cortex upon posterior inferotemporal cortex during visuospatial learning.¹⁶

SEM is a *confirmatory* statistical approach; it assesses how well a model fits a given dataset. Several exploratory adaptations of SEM have been proposed. One method exhaustively tests and ranks every possible model that can be generated for a given data set.^{17,18} Another method initializes with zero paths and iteratively adds the path that would best improve model stability, continuing until including additional paths no longer significantly improve model stability.¹⁹ A third exploratory approach seeks to find consistent activations across subjects.²⁰

Spontaneous fluctuation in brain activity observed with fMRI (resting-state fMRI)

Motor studies of stroke patients in the MRI scanner present a number of practical problems.²¹ The first is unwanted head movement. Head motion causes errors in registration of voxel location to anatomic location, leading to both false-positive activation when there is task-correlated head motion and false-negative activation due to random motion introducing increased spatial noise in the MRI signal.²² Another problem encountered in patients with stroke is mirror movements.²¹ These are involuntary movements of the contralateral homologous body part. Their presence complicates interpretation of imaging studies of motor recovery because they are associated with activation in contralesional motor cortex.^{23,24}

One of the most promising paradigms in human neuroimaging is the study of slow (<0.1 Hz) fluctuations in the fMRI blood oxygen level dependent (BOLD) signal. Strong temporal correlations among neural systems exist even in the absence of overt task. This spontaneous activity (i.e., resting state) refers to activity that is not attributable to specific inputs or outputs; it represents activity that is intrinsically generated by the brain. Although the physiological source of this spontaneous activity is unclear, it arises in functionally

associated regions, for example, components of the motor network.²⁵ Thus, this activity is thought to represent underlying neuronal activity within these networks. Evidence for the neuronal nature of the resting-state networks comes from studies that employ simultaneous fMRI and electroencephalograms (EEGs),^{26,27} from the observations of altered connectivity caused by neurological diseases,²⁸ and from the existence of homologous resting-state networks in nonhuman primates that overlap with neuroanatomically defined systems.²⁹ For a complete description of the theoretical framework for studying spontaneous activity and methodology, see reviews by Buckner et al³⁰ and Fox and Raichle.³¹

An application of resting-state BOLD that is likely to yield good results is the comparison of correlation patterns between groups. Task-based analyses face many confounds, including task-induced head motion, differences in task performance, task-correlated head movements, and different strategies for task completion. Task-based comparisons of movement-impaired stroke populations to control groups, or assessment of the neural correlates of functional recovery after stroke, face the additional confounds of mirror movements and differences in task difficulty due to severity of impairment. There are fewer assumptions needed when analyzing resting-state data, which makes group comparison much less problematic. Additionally, as there is **no task**, studies can be conducted in people unwilling or unable to adhere to task paradigms. Resting-state data have been shown to be remarkably consistent across sessions in healthy individuals,^{32,33} implying that network analysis would be useful in following longitudinal treatment-related manipulations. Furthermore, resting-state networks appear to be little changed by an intervening cognitive task in the course of a single scan session.³⁴ Recently, pathological disturbances in intrinsic resting-state activity have been related to the severity of disease³⁵⁻³⁷ and the recovery from functional deficits in stroke.³⁵

In addition to predicting how brain regions will respond to a task, spatial patterns of spontaneous activity may also predict an individual's task performance or behavior. Specifically, individual differences in the spatial topography of spontaneous activity have been shown to correspond to individual differences in prescan anxiety³⁸ and performance on working memory tasks.³⁹ The idea that an individual's spontaneous brain activity may predict that person's behavior for a particular task promises to be a major focus for future research.

Previous studies have shown that major human cortical networks exhibit correlated spontaneous activity while people are at rest.^{29,40,41} Networks subserving vision, motor control, and hearing show robust resting-state functional connectivity in healthy adults and even infants.⁴² Vincent and colleagues²⁹ provided the first evidence that such activity is neither restricted to the human brain nor tied to a conscious state. Their findings suggest that fluctuations of spontaneous activity across anatomically interconnected brain regions constitute a fundamental principle of brain organization. Such an interpretation is supported by the fact that organized patterns of brain activity are present in both humans and nonhuman primates. As to the functional significance of correlated signal fluctuations, it may be that they maintain the integrity of networks by reinforcing the synaptic connections between neurons that are essential for network operations in the awake state. Indeed, in stroke patients, the effective connectivity of a brain network has been found to break down when one of its parts is damaged.³⁵ This loss of connectivity seemed to be correlated with the patients' behavioral impairments.

The resting-state networks discussed thus far should not be confused with the default mode network (DMN), which has received increased attention in recent years.^{43,44} DMN principally includes the posterior cingulate, bilateral parietal lobe, ventromedial prefrontal cortex, and subgenual cingulate. The precise cognitive function of the DMN is unknown,

although it has been speculated as being engaged in self-referential activities such as daydreaming or rumination.⁴³ DMN is anti-correlated with cognitively demanding tasks, such as a visuospatial working memory task.⁴⁴ DMN also shows strong functional connectivity during resting-state scans. We urge readers not to mistake the DMN, which shows strong correlation during rest, with networks subserving other cognitive functions (such as motor control, vision, and audition), which also show correlated spontaneous activity during rest.

Assessing effective connectivity in stroke recovery

Only one other study has investigated changes in effective connectivity with stroke. Relative to healthy controls, stroke survivors have previously demonstrated disrupted motor network effective connectivity. Grefkes et al⁴⁵ showed a diminished influence of supplementary motor area (SMA) upon ipsilesional primary motor area (MI) independent of task performance. They also reported an increased inhibitory influence of contralesional to ipsilesional MI that was commensurate with extent of motor task impairment.

In the present study, we used an exploratory adaptation of SEM to evaluate changes in effective connectivity in the motor network of stroke survivors with rehabilitative therapy. Given the findings of Grefkes et al, we hypothesize that a lesion caused by an event such as a stroke would significantly diminish the driving influences of the affected hemisphere. Thus, the stroke-affected hemisphere would be overly reliant upon (and thus heavily influenced by) the unaffected hemisphere prior to therapy. But as the patient recovers motor function in the affected hand, we expect the stroke-affected hemisphere to reassert itself in the motor network. As a result, we expect the affected hemisphere to be less dependent upon the unaffected hemisphere following therapy. Specifically, we anticipate a reversal of the trends previously reported by Grefkes et al, as the brain recovers to more closely resemble that of healthy controls.

Methods

Patients

Accelerated Skill Acquisition Program (ASAP) group—We studied five right-handed patients (mean age 55 years) with recent strokes as confirmed by MRI or computed tomography (CT). Three patients had right hemiparesis due to infarctions located in the basal ganglia, pons, or thalamus. The other two patients presented with left hemiparesis resulting from a thalamic infarct or hemorrhage into the posterior limb of the internal capsule (PLIC). Stroke latency ranged from 34 to 55 days before baseline evaluation. Demographic data for this cohort are reported in Table 1. Each participant gave informed consent. The study was approved by the institutional review boards at each participating site (National Rehabilitation Hospital [NRH], Emory University [E], and the University of Southern California [USC]).

UCC patient—An additional right-handed patient (64 years) was recruited as a usual-and-customary-care control (UCC). This patient had a left thalamic stroke. This patient's demographic data are also reported in Table 1.

Control group—Two right-handed subjects (mean age 38 years) were recruited as a healthy control group. These subjects had no history of cerebrovascular events.

Behavioral assessments

Comparability and standardization of data collection techniques across all three sites were ensured prior to enrollment of subjects. Each participant underwent a detailed behavioral assessment prior to and immediately following 3 weeks of physical therapy⁴⁶ Each person was prescreened using the Orpington Prognostic Scale,⁴⁷ the National Institutes of Health Stroke Scale (NIHSS),⁴⁸ the Mini-Mental State Examination (MMSE),⁴⁹ and the Barthel Index.⁵⁰ Primary outcome measures included the Wolf Motor Function Test (WMFT)⁵¹ and the upper extremity portion of the Fugl-Meyer.⁵² Secondary measures included the Stroke Impact Scale (SIS),⁵³ the 9-item self-report Patient Health Questionnaire-9,^{54,55} and the 20-item Confidence in Arm and Hand Movements scale (CAHM), a measure of self-efficacy.

Rehabilitation intervention

ASAP—Task-specific functional training focused on the systematic and repetitive practice of tasks that could be performed with the level of available voluntary arm function. Tasks were progressively arranged and customized to account for any unique proximal-to-distal recovery patterns of reaching and grasping actions. All tasks were designed to be standard and repeatable and to have some functional goal (e.g., pointing, grasping, and stirring). The principles of motor learning were applied as the physical therapists systematically provided knowledge of results and progressed task difficulty to keep the participants challenged, motivated, and engaged.⁵⁶ Tasks were ordered randomly during practice to facilitate learning and to mimic real-world activities.⁵⁷ Therapy was provided at a dose of 2 hours a day, 5 days a week for 3 weeks (30 hours). Therapy was administered one-on-one by an experienced clinical therapist.

UCC—Patient underwent physician-prescribed rehabilitation therapy.

Control—Participants had no therapy or task practice between scanning sessions.

Magnetic resonance imaging

Subjects received two MRI sessions (one before and one after therapy). Each session included two resting-state fMRI (rs-fMRI) scans (TR/TE/FA=1500ms/30ms/90°, 200 time points [5 min each], resolution=3.4 × 3.4 × 5 mm³, 21 axial slices) on a Siemens 3.0T Magnetom Trio scanner (Siemens Medical Solutions, USA). Each rs-fMRI scan was preceded by a 150-s motor task functional scan. The motor task scans used a block design paradigm consisting of alternating 30-s periods of rest and performance of an isometric precision grip task. All functional data sets underwent motion correction, slice timing correction, scaling to percent signal change, bandpass temporal filtering (0.009–0.08 Hz), and then transformation to the ICBM452 anatomic brain template using previously described methods.⁵⁸

Region of interest (ROI) definitions are illustrated in Figure 1. First, the left hemisphere primary motor area was identified by its distinctive “hand knob” anatomic landmark (indicated by the arrow and contour tracing in Figure 1A).⁶ A 6-mm radius sphere was placed atop the hand knob and used as a seed for generating a correlation map using the rs-fMRI scans (Figure 1B). This correlation map guided the placement of 5 ROIs (also using 6-mm radius spheres; see Figure 1C): left and right M1 (LM1, RM1), left and right lateral dorsal premotor (LPM, RPM), and supplementary motor area (SMA). For all subjects, the seed maps generated for session 1 overlapped those generated for session 2. Thus, the same ROIs (generated for session 1) were used for both session 1 and session 2 to ensure consistency in data analysis across sessions.

ROI placement was performed by an investigator (G.A.J.) blind to which hemisphere was affected by stroke. As such, the distinction of *left* and *right* was necessary for anatomic definition. For clarity, results henceforth will be discussed only in terms of *affected* or *unaffected* hemisphere. Premotor and M1 ROIs in the hemisphere *affected* by the stroke will be referred to as *a*-PM and *a*-M1 respectively, while premotor and M1 ROIs in the *unaffected* hemisphere will be referred to as *u*-PM and *u*-M1.

Exploratory SEM was conducted using LISREL 8.80 (SSI, Inc., Lincolnwood, Illinois, USA) as previously described.¹⁹ SEM generates linear equations describing relationships among the variables of interest (for this work, ROI activity timecourses). These relationships are often depicted as paths with arrows indicating the *direction of influence* and path coefficients reflecting the *strength of influence*. The path coefficient of A to B indicates by how many standard deviation units B increases corresponding to an increase of 1 standard deviation units in A. For our exploratory adaptation, SMA was selected as an exogenous variable (i.e., node with only outputs to other nodes), thus serving as the network's starting point, while both M1 nodes were constrained to only have outputs to each other, thus establishing a hierarchy of SMA to PM to M1 that has been well documented for motor execution and motor imagery^{18,59} We used LISREL's automatic model modification procedure, which began with no paths estimated and used the modification index to choose which path would best stabilize the model if estimated. The process iteratively estimated the paths until the improvement in model stability (as measured by decreases in the chi-squared value) was no longer significant.¹⁹ Since the alpha (intercept) matrix was consistently near zero for all models, we fixed alpha to zero to free up degrees of freedom. This improved each model's parsimonious goodness-of-fit (PGFI) and allowed more paths to be estimated.

Results

Behavioral data

Table 1 shows pre- and posttreatment scores in functional performance on the primary outcome measures. The mean change ($\pm SD$) on the WMFT was 51.6 ± 30.8 , and the Fugl-Meyer affected arm score was 13.6 ± 13.9 . Large improvements in scores of self-efficacy (CAHM) were observed in three of five patients. Quality of life measurements (SIS scores 11.6 ± 6.1) were recorded only at baseline.

Resting-state effective connectivity

All models generated by this exploratory SEM approach met statistical criteria for validity. All models had a standardized root-mean-square residual (stRMR) < 0.02 , root-mean-square error of approximation (RMSEA) < 0.01 , and adjusted goodness-of-fit index (AGFI) 0.98.

For all five ASAP patients, the influence of *a*-PM to *u*-PM increased after therapy (Figure 2). For ASAP-01, *a*-PM had a strong influence on *u*-PM before therapy (path coefficient of 0.55), but this influence increased (0.66) after therapy. ASAP-02 showed a reversal in premotor influence, with *u*-PM driving *a*-PM before therapy (as exhibited by a path coefficient of 0.53) but *a*-PM driving *u*-PM afterwards (0.89). ASAP-03 was similar to patient 1, with *a*-PM's influence on *u*-PM increasing (albeit marginally) after therapy. ASAP-04 exhibited no interaction between premotor cortices before therapy but a remarkably strong influence (0.96) of *a*-PM on *u*-PM afterwards. ASAP-05 showed an influence of SMA on all four ROIs pre therapy but no interregional influence; this changed post therapy, where *a*-PM and *u*-PM showed strongly reciprocating path coefficients indicative of high correlation. The three patients with the greatest change in WMFT scores (ASAP-01, ASAP-02, ASAP-04) also had the greatest change in influence of *a*-PM upon *u*-

PM with therapy. Conversely, UCC-01 showed the opposite pattern: *u*-PM influenced *a*-PM both before and after therapy, with no reciprocal influence of *a*-PM upon *u*-PM.

For four patients, the influence of *a*-PM on *a*-M1 increased after therapy. Three patients (ASAP-01, ASAP-03, UCC-01) showed no influence of *a*-PM on *a*-M1 pre therapy but strong influence post therapy. One patient (#2) showed a decreasing direct influence of *a*-PM on *a*-M1 pre to post therapy (-0.11 to 0) but an increased indirect influence (*a*-PM to *u*-PM to *a*-M1 to *a*-M1; total indirect influence 0.55), resulting in a net increase. Only one patient (#4) had decreased influence of *a*-PM on *a*-M1 (0.26 to 0).

The two patients with greatest behavioral improvement (ASAP-01 and ASAP-02) were also the only two patients showing an increased influence of SMA on *a*-PM after therapy. These patients showed no direct influence of SMA on *a*-M1 post therapy, that is, SMA could only influence *a*-M1 indirectly through *a*-PM. Three patients (ASAP-04, ASAP-05, UCC-01) showed the opposite trend; SMA on *a*-PM decreased with time, and SMA had a direct connection to *a*-M1 post therapy. The patient with the least behavioral improvement (ASAP-03) had no change in SMA's influence on *a*-PM with therapy and no direct influence of SMA upon *a*-M1 pre or post therapy.

The control participants had consistent influence of SMA upon LPM and LPM upon RPM, for both sessions. Both subjects were right-handed, suggesting an influence of the dominant (left) hemisphere over the nondominant (right) hemisphere.

Each session's resting scans were preceded by (and thus separated by) the motor task scan, so that the task between resting scans may have induced motor network priming. This was ruled out by a paired sample *t* test, which found no significant difference between Fisher *z*-transformed correlations on the first and second resting-state scans ($p < .05$) for either pre- or posttherapy sessions.

Discussion

We have documented longitudinal changes in effective connectivity bilaterally in the motor network, corresponding with improved motor function of the stroke-affected upper limb following therapy. All ASAP patients demonstrated increased effective connectivity from *a*-PM to *u*-PM, with the magnitude of connectivity increase being proportional to behavioral measures of recovery. The reciprocal relationship (influence from *u*-PM to *a*-PM) increased only for patient 5; for all other patients, this influence remained at zero (patients 1, 3, 4) or decreased (patient 2). To our knowledge, these findings are the first to suggest that the increased effective connectivity from affected to unaffected PM is not merely a return to the bilaterality typically observed in the resting-state motor network,⁶⁰ but rather reflects functional reorganization of the motor network following stroke.

UCC-01 showed no increase of *a*-PM upon *u*-PM with therapy; *u*-PM influenced *a*-PM both pre and post therapy. Conversely, the influence of *u*-PM upon *a*-PM before therapy persisted after therapy. Yet UCC-01 had moderate behavioral improvement, suggesting that the influence of *a*-PM upon *u*-PM may be a therapy-specific neural correlate of functional recovery. Differing rehabilitative therapies may "retrain" the brain in different ways, thus inducing different neural plasticities. SEM could hence investigate how different therapies differentially reorganize neural connectivity, with unique paths serving as therapy-specific indicators of efficacy. Although intriguing, such speculation requires further empirical evaluation.

A strong intrahemispheric influence of PM to M1 has been reported in normal populations.^{18,59} Four patients in the current study showed increased influence of *a*-PM to *a*-

M1 across sessions, including the two with greatest motor improvement. This increase is consistent with motor recovery, as it suggests a re-establishment of influences observed in unimpaired people. The changing role of SMA with stroke recovery is less clear. The two patients with greatest recovery showed a tendency for SMA to directly influence *a*-M1 pre therapy but to reroute to affect *a*-PM post therapy. Although this rerouting may reflect neural plasticity with motor recovery, a larger sample is again needed to fully explore this relationship.

Modeling patients individually is a necessary step for understanding the heterogeneity of cortical activity during recovery of stroke survivors⁶¹ and for monitoring treatment effects in patients. Both the investigator (G.A.J.) and the algorithm were blind to which hemisphere was affected by stroke, yet the modeling approach consistently showed increased influence of *a*-PM on *u*-PM across all subjects. These results suggest recruitment of the unaffected hemisphere to aid the affected hemisphere, which is consistent with our hypothesis as well as previous findings.⁶² Additional factors (such as standardized changes in influence between regions) could be extracted from the models to serve as predictors for stroke recovery. While prognostic applications of SEM are beyond the scope of this paper, we have laid out the framework within which such investigations could be attempted. Future work will apply this methodology across patients receiving multiple therapeutic approaches using appropriate control groups. Thus, neuroimaging may allow us to predict not only how a patient may generally recover but also guide the choice of therapy that would maximally benefit the patient.

A comparison of control subjects to stroke patients is complicated by control subjects not having a neurologically affected hemisphere. Additionally, the two control subjects were younger than the ASAP patients, so an age-matched cohort would be necessary to make proper comparisons. Nonetheless, a consistent pattern was observed for control subjects: SMA affects LPM and LPM affects RPM in both sessions. Since both control subjects were right-handed, an influence of LPM upon RPM is not unexpected. These two paths were also present for an exploratory model derived from healthy subjects performing a bimanual motor task.¹⁸ While the coefficients for these paths varied considerably, their *t* scores ranged from 8 to 30, indicating robustness.

Conclusions

Our findings support the hypothesis that, following stroke, the unaffected hemisphere strongly influences the affected hemisphere and that this influence reverses with recovery. Even though the results are encouraging, the small sample size curtails what inferences can reasonably be drawn. Future studies with larger samples would allow for investigation of specific influences on rehabilitation, for example, how motor network connectivity varies with subcortical versus cortical lesions or with paresis of the dominant versus nondominant hand. Future applications of this technique may provide imaging metrics, in addition to behavioral outcomes, by which competing therapies may be evaluated or potentially by which the optimal therapy for a given patient may be chosen.

We additionally demonstrate that resting-state neuroimaging data can produce viable models of effective connectivity in the motor network within individual patients. Since these models are generated for individuals, they allow longitudinal assessment of patient recovery. Furthermore, specific network paths appear to correspond with behavioral measures of stroke recovery and are thus of potential prognostic value. Future effective connectivity analyses may identify key network paths that are critical for successful rehabilitation. In these instances, artificially restoring connectivity between these regions (e.g., with transcranial magnetic stimulation), independent of or in conjunction with rehabilitation

therapy, may facilitate motor skill restoration. Taking into account our findings of selective changes of resting-state networks in stroke, we suggest that resting-state fMRI and especially resting-state network analysis constitute very promising tools for the functional characterization of functional brain disorders, for intergroup comparisons, and possibly with some potential for assessing effective connectivity on a single subject level—all of which may have important implications for stroke rehabilitation.

Acknowledgments

This work was supported by National Institutes of Health grants RO1EB002009, K24EY017332, 1U01NS056256, and VA B4657P. We gratefully acknowledge the work of the physical therapists and evaluators. We thank the clinical site principal investigators Drs. C. Winstein, S. Wolf, and A. Dromerick. Special thanks to J. Rajendra for his work on the data collection and Dr. J. Craggs for assistance in refining the SEM analysis. Dr. Hu is supported by grants from The National Institutes of Health and is currently a consultant of ZhuHai Hejia Medical instruments.

References

1. Rosamond W, Flegal K, Friday G, et al. Heart disease and stroke statistics–2007 update: a report from the American Heart Association Statistics Committee and Stroke Statistics Subcommittee. *Circulation*. 2007; 115(5):e69–171. [PubMed: 17194875]
2. Catalan MJ, Honda M, Weeks RA, Cohen LG, Hallett M. The functional neuroanatomy of simple and complex sequential finger movements: a PET study. *Brain*. 1998; 121(Pt 2):25364.
3. Deiber MP, Passingham RE, Colebatch JG, Friston KJ, Nixon PD, Frackowiak RS. Cortical areas and the selection of movement: a study with positron emission tomography. *Exp Brain Res*. 1991; 84(2):393–402. [PubMed: 2065746]
4. Grafton ST, Mazziotta JC, Presty S, Friston KJ, Frackowiak RS, Phelps ME. Functional anatomy of human procedural learning determined with regional cerebral blood flow and PET. *J Neurosci*. 1992; 12(7):2542–2548. [PubMed: 1613546]
5. Jenkins IH, Brooks DJ, Nixon PD, Frackowiak RS, Passingham RE. Motor sequence learning: a study with positron emission tomography. *J Neurosci*. 1994; 14(6):3775–3790. [PubMed: 8207487]
6. Yousry TA, Schmid UD, Alkadhi H, et al. Localization of the motor hand area to a knob on the precentral gyrus. A new landmark. *Brain*. 1997; 120(Pt1):141–157. [PubMed: 9055804]
7. Toni I, Krams M, Turner R, Passingham RE. The time course of changes during motor sequence learning: a whole-brain fMRI study. *NeuroImage*. 1998; 8(1):50–61.
8. He AG, Tan LH, Tang Y, et al. Modulation of neural connectivity during tongue movement and reading. *Hum Brain Mapping*. 2003; 18(3):222–232.
9. Hansen LK, Larsen J, Nielsen FA, et al. Generalizable patterns in neuroimaging: how many principal components? *NeuroImage*. 1999; 9(5):534–544.
10. Moeller JR, Strother SC. A regional covariance approach to the analysis of functional patterns in positron emission tomographic data. *J Cereb Blood Flow Metab*. 1991; 11 (2):A121–135. [PubMed: 1997480]
11. McIntosh AR, Bookstein FL, Haxby JV, Grady CL. Spatial pattern analysis of functional brain images using partial least squares. *NeuroImage*. 1996; 3 (3Pt 1):143–157.
12. McKeown MJ, Jung TP, Makeig S, et al. Spatially independent activity patterns in functional MRI data during the Stroop color-naming task. *Proc Natl Acad Sci USA*. 1998; 95(3):803–810. [PubMed: 9448244]
13. McKeown, Mj; Makeig, S.; Brown, GG., et al. Analysis of fMRI data by blind separation into independent spatial components. *Hum Brain Mapping*. 1998; 6(3):160–188.
14. McIntosh AR, Gonzalez-Lima F. Structural modeling of functional neural pathways mapped with 2-deoxyglucose: effects of acoustic startle habituation on the auditory system. *Brain Res*. 1991; 547(2):295–302. [PubMed: 1884204]
15. Buchel C, Friston KJ. Modulation of connectivity in visual pathways by attention: cortical interactions evaluated with structural equation modelling and fMRI. *Cereb Cortex*. 1997; 7(8): 768–778. [PubMed: 9408041]

16. Buchel C, Coull JT, Friston KJ. The predictive value of changes in effective connectivity for human learning. *Science*. 1999; 283(5407):1538–1541. [PubMed: 10066177]
17. James GA, Kelley ME, Craddock RC, et al. Exploratory structural equation modeling of resting-state fMRI: applicability of group models to individual subjects. *NeuroImage*. 2009; 45:778–787.
18. Zhuang J, LaConte S, Peltier S, Zhang K, Hu X. Connectivity exploration with structural equation modeling: an fMRI study of bimanual motor coordination. *NeuroImage*. 2005; 25(2):462–470.
19. Craggs JG, Price DD, Verne GN, Perlstein WM, Robinson MM. Functional brain interactions that serve cognitive-affective processing during pain and placebo analgesia. *NeuroImage*. 2007; 38(4): 720–729.
20. Glen, DR.; Chen, G. [Accessed 2007] Structural Equation Modeling (SEM) or Path Analysis in AFNI. Available at: <http://afni.nimh.nih.gov/sscc/gangc/PathAna.html>
21. Krakauer JW. Functional imaging of motor recovery after stroke: remaining challenges. *Curr Neurol Neurosci Rep*. 2004; 4(1):42–46. [PubMed: 14683627]
22. Jezzard, P.; Matthews, PM.; Smith, SM. *Functional MRI: An Introduction to Methods*. Vol. xiii. Oxford, New York: Oxford University Press; 2001. p. 390
23. Kim YH, Jang SH, Chang Y, Byun WM, Son S, Ahn SH. Bilateral primary sensori-motor cortex activation of post-stroke mirror movements: an fMRI study. *Neuroreport*. 2003; 14(10):1329–1332. [PubMed: 12876467]
24. Wittenberg GF, Bastian AJ, Dromerick AW, Thach WT, Powers WJ. Mirror movements complicate interpretation of cerebral activation changes during recovery from subcortical infarction. *Neurorehabil Neural Repair*. 2000; 14(3):213–221. [PubMed: 11272478]
25. Biswal B, Yetkin FZ, Haughton VM, Hyde JS. Functional connectivity in the motor cortex of resting human brain using echo-planar MRI. *Magn Reson Med*. 1995; 34(4):537–541. [PubMed: 8524021]
26. Laufs H, Kleinschmidt A, Beyerle A, et al. EEG-correlated fMRI of human alpha activity. *Neuroimage*. 2003; 19(4):1463–1476. [PubMed: 12948703]
27. Mantini D, Perrucci MG, Del Gratta C, Romani GL, Corbetta M. Electrophysiological signatures of resting state networks in the human brain. *Proc Natl Acad Sci USA*. 2007; 104(32):13170–13175. [PubMed: 17670949]
28. Greicius MD, Srivastava G, Reiss AL, Menon V. Default-mode network activity distinguishes Alzheimer’s disease from healthy aging: evidence from functional MRI. *Proc Natl Acad Sci USA*. 2004; 101 (13):4637–4642. [PubMed: 15070770]
29. Vincent JL, Patel GH, Fox MD, et al. Intrinsic functional architecture in the anaesthetized monkey brain. *Nature*. 2007; 447(7140):83–86. [PubMed: 17476267]
30. Buckner RL, Andrews-Hanna JR, Schacter DL. The brain’s default network: anatomy, function, and relevance to disease. *Ann NY Acad Sci*. 2008; 1124:1–38. [PubMed: 18400922]
31. Fox MD, Raichle ME. Spontaneous fluctuations in brain activity observed with functional magnetic resonance imaging. *Nat Rev Neurosci*. 2007; 8(9):700–711. [PubMed: 17704812]
32. Damoiseaux JS, Rombouts SA, Barkhof F, et al. Consistent resting-state networks across healthy subjects. *Proc Natl Acad Sci USA*. 2006; 103(37):13848–13853. [PubMed: 16945915]
33. Chen S, Ross TJ, Zhan W, et al. Group independent component analysis reveals consistent resting-state networks across multiple sessions. *Brain Res*. 2008; 1239(6):141–151. [PubMed: 18789314]
34. Waites AB, Stanislavsky A, Abbott DF, Jackson GD. Effect of prior cognitive state on resting state networks measured with functional connectivity. *Hum Brain Mapping*. 2005; 24(1):59–68.
35. He BJ, Snyder AZ, Vincent JL, Epstein A, Shulman GL, Corbetta M. Breakdown of functional connectivity in frontoparietal networks underlies behavioral deficits in spatial neglect. *Neuron*. 2007; 53(6):905–918. [PubMed: 17359924]
36. Greicius MD, Flores BH, Menon V, et al. Resting-state functional connectivity in major depression: abnormally increased contributions from subgenual cingulate cortex and thalamus. *Biol Psychiatry*. 2007; 62(5):429–437. [PubMed: 17210143]
37. Bluhm RL, Miller J, Lanius RA, et al. Spontaneous low-frequency fluctuations in the BOLD signal in schizophrenic patients: anomalies in the default network. *Schizophr Bull*. 2007; 33(4):1004–1012. [PubMed: 17556752]

38. Seeley WW, Menon V, Schatzberg AF, et al. Dissociable intrinsic connectivity networks for salience processing and executive control. *J Neurosci*. 2007; 27(9):2349–2356. [PubMed: 17329432]
39. Hampson M, Driesen NR, Skudlarski P, Gore JC, Constable RT. Brain connectivity related to working memory performance. *J Neurosci*. 2006; 26(51):13338–13343. [PubMed: 17182784]
40. Biswal BB, Van Kylen J, Hyde JS. Simultaneous assessment of flow and BOLD signals in resting-state functional connectivity maps. *NMR Biomed*. 1997; 10(4–5):165–170. [PubMed: 9430343]
41. Fox MD, Corbetta M, Snyder AZ, Vincent JL, Raichle ME. Spontaneous neuronal activity distinguishes human dorsal and ventral attention systems. *Proc Natl Acad Sci USA*. 2006; 103(26):10046–10051. [PubMed: 16788060]
42. Fransson P, Skiold B, Horsch S, et al. Resting-state networks in the infant brain. *Proc Natl Acad Sci USA*. 2007; 104(39):15531–15536. [PubMed: 17878310]
43. Fox MD, Snyder AZ, Vincent JL, Corbetta M, Van Essen DC, Raichle ME. The human brain is intrinsically organized into dynamic, anticorrelated functional networks. *Proc Natl Acad Sci USA*. 2005; 102(27):9673–9678. [PubMed: 15976020]
44. Greicius MD, Krasnow B, Reiss AL, Menon V. Functional connectivity in the resting brain: a network analysis of the default mode hypothesis. *Proc Natl Acad Sci USA*. 2003; 100(1):253–258. [PubMed: 12506194]
45. Grefkes C, Eickhoff SB, Nowak DA, Dafotakis M, Fink GR. Dynamic intra- and interhemispheric interactions during unilateral and bilateral hand movements assessed with fMRI and DCM. *NeuroImage*. 2008; 41 (4):1382–1394.
46. Winstein CJ, Rose DK, Tan SM, Lewthwaite R, Chui HC, Azen SP. A randomized controlled comparison of upper-extremity rehabilitation strategies in acute stroke: a pilot study of immediate and long-term outcomes. *Arch Phys Med Rehabil*. 2004; 85(4):620–628. [PubMed: 15083439]
47. Kalra L, Potter J, Patel M, McCormack P, Swift CG. The role of standardised assessments in comparing stroke unit rehabilitation. *Cerebrovasc Dis*. 1997; 7:77–84.
48. Bates B, Choi JY, Duncan PW, et al. Veterans Affairs/Department of Defense Clinical Practice Guideline for the Management of Adult Stroke Rehabilitation Care: executive summary. *Stroke*. 2005; 36(9):2049–2056. [PubMed: 16120847]
49. Folstein MF, Folstein SE, McHugh PR. “Mini-mental state”. A practical method for grading the cognitive state of patients for the clinician. *J Psychiatr Res*. 1975; 12(3):189–198. [PubMed: 1202204]
50. Mahoney FI, Barthel DW. Functional evaluation: The Barthel Index. *Md State Med J*. 1965; 14:61–65. [PubMed: 14258950]
51. Wolf SL, Catlin PA, Ellis M, Archer AL, Morgan B, Piacentino A. Assessing Wolf Motor Function Test as outcome measure for research in patients after stroke. *Stroke*. 2001; 32(7):1635–1639. [PubMed: 11441212]
52. Fugl-Meyer AR, Jaasko L, Leyman I, Olsson S, Steglind S. The post-stroke hemiplegic patient. 1. a method for evaluation of physical performance. *Scand J Rehabil Med*. 1975; 7(1):13–31. [PubMed: 1135616]
53. Duncan PW, Wallace D, Lai SM, Johnson D, Embretson S, Laster LJ. The stroke impact scale version 2.0. Evaluation of reliability, validity, and sensitivity to change. *Stroke*. 1999; 30(10): 2131–2140. [PubMed: 10512918]
54. Lowe B, Unutzer J, Callahan CM, Perkins AJ, Kroenke K. Monitoring depression treatment outcomes with the patient health questionnaire-9. *Med Care*. 2004; 42(12):1194–1201. [PubMed: 15550799]
55. Williams LS, Brizendine EJ, Plue L, et al. Performance of the PHQ-9 as a screening tool for depression after stroke. *Stroke*. 2005; 36(3):635–658. [PubMed: 15677576]
56. Winstein, CJ. Motor learning considerations in stroke rehabilitation. In: Duncan, PW.; Badke, MB., editors. *Stroke Rehabilitation: The Recovery of Motor Control*. Chicago: Year Book Medical; 1987. p. 109-34.
57. Hanlon RE. Motor learning following unilateral stroke. *Arch Phys Med Rehabil*. 1996; 77(8):811–815. [PubMed: 8702377]

58. James GA, Kelley ME, Craddock RC, et al. Exploratory structural equation modeling of resting-state fMRI: applicability of group models to individual subjects. *NeuroImage*. 2009; 45:778–787.
59. Solodkin A, Hlustik P, Chen EE, Small SL. Fine modulation in network activation during motor execution and motor imagery. *Cereb Cortex*. 2004; 14(11):1246–1255. [PubMed: 15166100]
60. Peltier SJ, Noll DC. T(2)(*) dependence of low frequency functional connectivity. *NeuroImage*. 2002; 16(4):985–992.
61. Johansen-Berg H. Functional imaging of stroke recovery: what have we learnt and where do we go from here? *Int J Stroke*. 2007; 2(1):7–16. [PubMed: 18705982]
62. Ward NS, Brown MM, Thompson AJ, Frackowiak RS. Neural correlates of motor recovery after stroke: a longitudinal fMRI study. *Brain*. 2003; 126 (Pt11):2476–2496. [PubMed: 12937084]

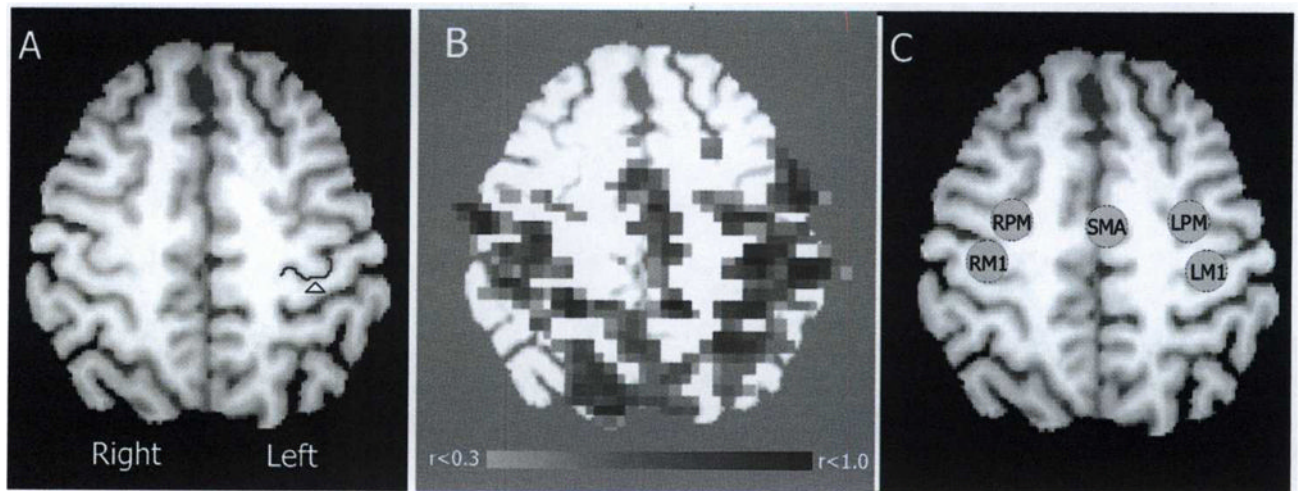


Figure 1.

Selection of regions of interest (ROIs). (A) Horizontal section of a T1 anatomic image of single patient's brain following transformation to MNI space ($z=50$ mm). Arrow and contour indicate the location of the left motor "hand knob." (B) A correlation map using left M1 as a seed is shown overlaid atop the T1 anatomic image. The thresholded ($0.3 < r < 1.0$) correlation map guided ROI placement. (C) Five ROIs: supplementary motor area (SMA), left and right lateral premotor (LPM, RPM), and left and right primary motor (LM1, RM1) were defined as 6-mm radius spheres set atop the T1 anatomic image.

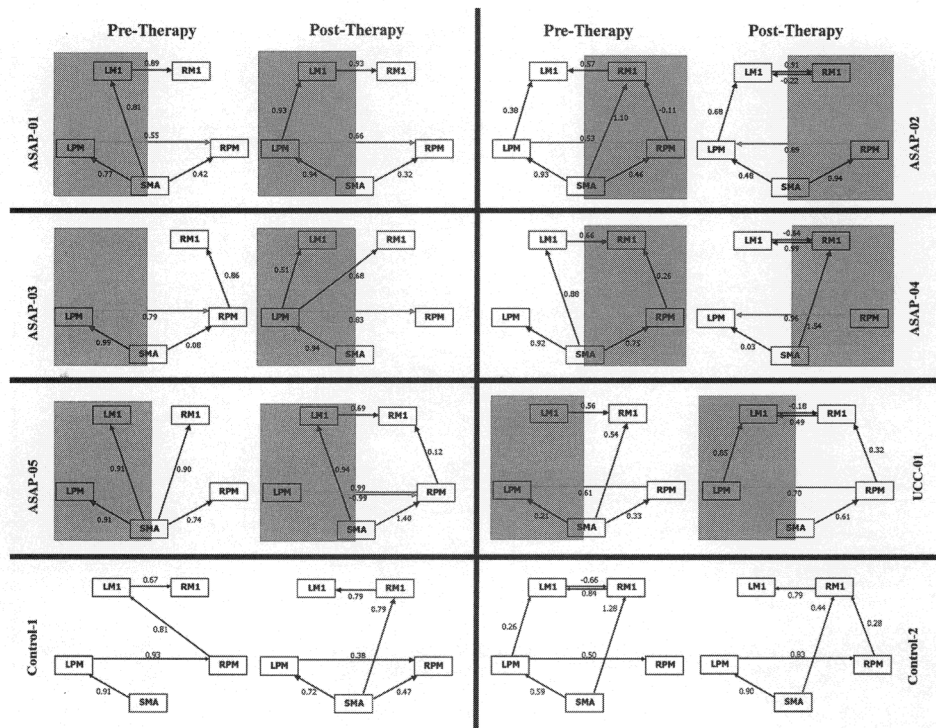


Figure 2. Motor system network for each stroke survivor, before (session 1) and after (session 2) therapy. Shading indicates the hemisphere that is affected by stroke. SEM models are shown for each patient's first session (left) and second session (right) after therapy. The numbers above each line represent the path coefficients and are standardized measures of direct influence. Solid lines with arrows indicate direction of effective connectivity influence. LM1=left primary motor cortex; RM1=right primary motor cortex; LPM = left premotor cortex; RPM=premotor cortex; SMA=supplementary motor area.

Table 1

Demographic and behavioral data

Subject	Patient 1 (ASAP)	Patient 2 (ASAP)	Patient 3 (ASAP)	Patient 4 (ASAP)	Patient 5 (ASAP)	Patient 6 (UCC)
Medical						
CVA lesion site (L/R)	L-CVA, pons, ischemic	R-CVA, PLIC, hemorrhagic	L-CVA basal ganglia	R-CVA medulla, ischemic	L-CVA, thalamus, ischemic	L-thalamic, hemorrhage
Dominant hand more affected	Yes	No	Yes	No	Yes	Yes
Comorbidities/past medical history/medications	HTN, HLP/depression/ metoprolol, Zocor, hydralazine, Diovan, amlodipine, Lexapro	HTN, DM, HLP/none/Novolin, lisinopril, Zocor, gemfibrozil	HTN, obesity/ETOH abuse/ aspirin, Plavix, Lipitor, lisinopril	Type II DM, HTN, HNP/C3-4 anterior midline with mild cord compression/none	None/gender reassignment 2001; trauma with coma; reconstruction 1985/Evamist	DM, HTN, CAD/none/Lexapro, Novolog, Altace, Lantus, Zocor, Glucophage
Demographics						
Race/ethnicity	African American	Asian American	Latin American	Caucasian American	Caucasian American	Caucasian American
Age	49	68	55	52	52	64
Gender	Male	Male	Male	Female	Female	Male
Marital status	S	M	M	S	Domestic partner	M
Timing						
Length of hospital stay, days	27	18	WHC17 NRH8	23	28	27
Screen, days since stroke onset	10	13	25	21	27	20
Baseline evaluation, days since onset	55	38	35	36	34	64
Post evaluation	85	68	62	58	55	83
Screen						
Orpington Prognostic Scale	10	9	NT	2.4	2.8	NT
NIHSS	1	4	6	4	5	4
MMSE	29	NA	NT	NT	NT	—
Barthel Index prior to stroke	100	100	100	NT	NT	100
Evaluation						
Treatment	ASAP	ASAP	ASAP	ASAP	ASAP	UCC
Fugl-Meyer baseline	42	39	54	34	53	37
Fugl-Meyer post intervention	44	43	59	47	56	41
Baseline WMFT affected, average time in seconds	21.29	28.69	5.28	4.499	4.25	5.31
Post WMFT affected, average time in seconds	4.53	2.98	3.81	2.652	3.37	3.82
SIS hand, sum (average)	8 (1.6)	5(1)	17(3)	9	19	19
Brief self-efficacy (initial/final)	1/5.5	5/9	5/8-	NT	NT	NT

Subject	Patient 1 (ASAP)	Patient 2 (ASAP)	Patient 3 (ASAP)	Patient 4 (ASAP)	Patient 5 (ASAP)	Patient 6 (UCC)
Baseline CAHM, average	26	6.25	66.75	NT	NT	32.5
Postintervention CAHM, average	51	47	70	NT	NT	71
PHQ-9 baseline	13	NT	NT	NT	NT	2
PHQ-9 post intervention	12	NT	NT	NT	NT	3

Note: ASAP=Accelerated Skill Acquisition Program; UCC=usual-and-customary control; PLJC=posterior limb of internal capsule; HTN=hypertension; HLP=hyperlipoproteinemia; DM=diabetes mellitus; S=single; M=married; WHC=Washington Health Center; NRH=National Rehabilitation Hospital; NT=not tested; NIHSS=National Institutes of Health Stroke Scale; NA=not available; MMSE=Mini Mental State Examination; WMFT=Wolf Motor Function Test; SIS=Stroke Impact Scale; CAHM=Confidence in Arm and Hand Movements Scale; PHQ-9=9-item Patient Health Questionnaire.